普通高等教育“十三五”规划教材

孙萌涛　李源作　编著
Sun Mengtao　Li Yuanzuo

One- and Two- Photon Absorptions: Principles and Applications

单光子和双光子吸收：原理和应用

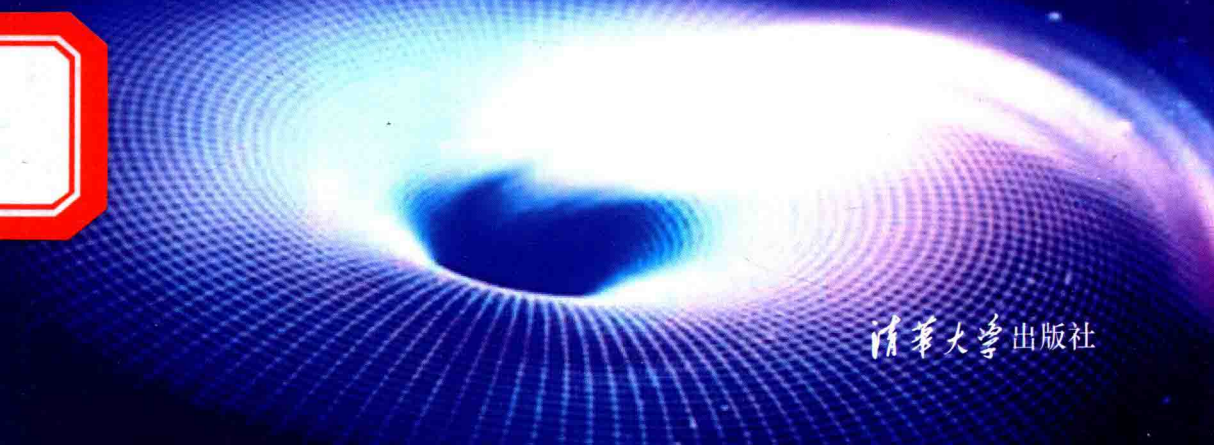

清华大学出版社

One- and Two- Photon Absorptions: Principles and Applications

单光子和双光子吸收：原理和应用

孙萌涛　李源作　编著
Sun Mengtao　Li Yuanzuo

清華大學出版社
北京

内 容 简 介

本教材共分为9章，系统介绍了单光子吸收理论，单光子诱导电子空穴相关性，在生物、材料、SERS中的单光子过程，双光子吸收理论，非线性极化率理论，双光子诱导电子空穴相关性和双光子荧光分子应用等内容。本书内容深入浅出，通俗易懂。

本教材适用于物理学、光学、化学、材料学等专业科研院所和高校的研究人员、研究生及高年级本科生使用。

版权所有，侵权必究。侵权举报电话：010-62782989　13701121933

图书在版编目(CIP)数据

单光子和双光子吸收：原理和应用：英文/孙萌涛，李源作编著. —北京：清华大学出版社，2018

ISBN 978-7-302-49974-9

Ⅰ. ①单… Ⅱ. ①孙… ②李… Ⅲ. ①光电子技术—英文 ②双光子吸收—英文 Ⅳ. ①TN2 ②TN241

中国版本图书馆CIP数据核字(2018)第067461号

责任编辑：鲁永芳
封面设计：常雪影
责任校对：赵丽敏
责任印制：刘海龙

出版发行：清华大学出版社
网　　址：http://www.tup.com.cn，http://www.wqbook.com
地　　址：北京清华大学学研大厦A座　　邮　　编：100084
社 总 机：010-62770175　　邮　　购：010-62786544
投稿与读者服务：010-62776969，c-service@tup.tsinghua.edu.cn
质量反馈：010-62772015，zhiliang@tup.tsinghua.edu.cn
印 装 者：北京泽宇印刷有限公司
经　　销：全国新华书店
开　　本：170mm×240mm　**印张**：11　**插页**：4　**字　　数**：223千字
版　　次：2018年4月第1版　　**印　　次**：2018年4月第1次印刷
定　　价：49.00元

产品编号：078549-01

Sun Mengtao, Li Yuanzuo

Sun Mengtao obtained his Ph. D. in 2003 from the State Key Laboratory of Molecular Reaction Dynamics, Dalian Institute of Chemical Physics, Chinese Academy of Sciences (CAS). From 2003 to 2006, he worked as a postdoc at the Department of Chemical Physics, Lund University. Since 2006, as an associate professor, he has worked at the Beijing National Laboratory for Condensed Matter Physics, Institute of Physics, Chinese Academy of Sciences(CAS). In 2016, he became a full professor in University of Science and Technology Beijing, China. His current research interests focus on one-and two-photon absorptions in organic molecules, two-dimensional (2D) materials and plasmonics, as well as the exciton-plasmon coupling interaction for surface catalytic reaction. He has published more than 150 papers, including 10 invited review papers, three books and three book chapters in English, and citations are about 5 000 times. Researcher ID: B1131-2008. In 2016, He was awarded the second prize of Science and Technology in Liaoning province.

Li Yuanzuo earned his Ph. D. in the School of Physics, Dalian University of Technology (DLUT) in 2011. He became an associate professor in Northeast Forestry University in 2014. His current research interests include: experiment and first principle calculation on solar cells, excited state dynamics, energy conversion and nanomaterials. He has published more than 60 scientific publications, reviews and book chapters in the field of excited state properties of organic systems.

CONTENTS

试读结束：需要全本请在线购买： www.ertongbook.com

CHAPTER 1

One-Photon Absorption Theory

It is known that there is a kind of electromagnetic(EM) interaction between light and matter, which determines the light absorption and the emission. Conjugated organic molecules have attracted considerable attention in the last decades due to their remarkable optoelectronic properties[1-6], and their structural malleability allows tunable optical properties, which can be exploited for different applications, such as optoelectronic and photonic devices[7-11]. The time-independent perturbation theory is considered as a way to deal with the above problem, and there is a case in which we want to study how systems respond to the imposed perturbations[12-15]. Firstly, we assume that the Hamiltonian H of the system can be written in the form:

$$\hat{H} = \hat{H}_0 + \lambda V \tag{1-1}$$

where, $\hat{H}_0$ is the Hamiltonian of the unperturbed system, and λV is a perturbation term applied to the system. Since H_0 is unperturbed, odinger equation is satisfied:

$$\hat{H}_0 \psi_n^0 = \mathrm{i}\hbar \frac{\partial \psi_n^0}{\partial t} \tag{1-2}$$

The wave functions ψ_n^0 are related to the time-dependent unperturbed wave-functions, as shown in form of $\psi_n^0 = \psi_n \exp(-\mathrm{i}tE_n/\hbar)$; while the whole system wave-functions $\psi(t)$ can be expressed as a linear combination of the ψ_n^0:

$$\psi = \sum_n C_n(t)\psi_n^0 \tag{1-3}$$

The time-dependent odinger equation containing the perturbation term of EM interaction is expressed as

$$(\hat{H}_0 + \lambda V)\psi = \mathrm{i}\hbar \frac{\partial \psi}{\partial t} \tag{1-4}$$

Inserting Eq.(1-3) into Eq.(1-4) gives

$$\lambda \sum_m C_m \langle \psi_n^0 \mid V \mid \psi_m^0 \rangle = \mathrm{i}\,\hbar \frac{\partial C_n}{\partial t} \tag{1-5}$$

Given the dipole interaction between a system and an electric field can be viewed as a very small quantity in comparison with the Hamiltonian without perturbation, the wave function of the system has only a small change; therefore, the coefficient C_n was defined as the $C_n = C_n^{(0)} + \lambda C_n^{(1)} + \lambda^2 C_n^{(2)} + \cdots$, where $C_n^{(1)}$ and $C_n^{(2)}$ were expansion coefficients of first- and second- order perturbations, respectively. And

$$\frac{\mathrm{d}C_n^{(0)}}{\mathrm{d}t} = 0 \tag{1-6}$$

$$\mathrm{i}\,\hbar \frac{\mathrm{d}C_n^{(1)}}{\mathrm{d}t} = \sum_m C_m^{(0)} \langle \Psi_n^0 \mid V \mid \Psi_m^0 \rangle \tag{1-7}$$

$$\mathrm{i}\,\hbar \frac{\mathrm{d}C_n^{(2)}}{\mathrm{d}t} = \sum_m C_m^{(1)} \langle \Psi_n^0 \mid V \mid \Psi_m^0 \rangle \tag{1-8}$$

Upon one electron is excited from initial state i, expanding coefficient $C_i^{(0)} = 1$. So

$$\mathrm{i}\,\hbar \frac{\mathrm{d}C_n^{(1)}}{\mathrm{d}t} = \langle \Psi_n^0 \mid V \mid \Psi_i^0 \rangle \tag{1-9}$$

$$C_n^{(1)} = (V_{fi} / \hbar\,\omega_{fi})(1 - \mathrm{e}^{\mathrm{i}\hbar\omega_{nk}}) \tag{1-10}$$

where $\omega_{fi} = (E_f - E_i)/\hbar$.

For one-photon absorption(OPA) or 1-photon absorption(1PA), also called single-photon absorption, transition probability per unit time from i state to f state is then given by

$$W_{i\to f}^{(1)} = \frac{|C_n^{(1)}|^2}{t} = \left(\frac{|V_{fi}|}{\hbar\,\omega_{fi}}\right)^2 (2 - 2\cos\omega_{fi}t) = \frac{2\pi}{\hbar} |V_{fi}|^2 \delta(E_f - E_i) \tag{1-11}$$

where V_{fi} is the perturbation matrix element. Considering the long interaction time between a system and an optical field, when $t \to +\infty$.

$$\delta(\omega_{fi}) = \frac{1}{\pi} \lim_{t\to\infty} \frac{1}{t} \frac{1 - \cos\omega t}{\omega_{nk}^2} \tag{1-12}$$

For calculating transition probability, each composite site, say initial state $|I\rangle$, is characterized by $|\varepsilon_i,\ n_L\,\hbar\omega, n_1\,\hbar\omega_2\rangle$; $|F\rangle \equiv |\varepsilon_f, (n_L - 1)\hbar\omega_1\rangle$, say final state. Furthermore, expanding the vector potential in terms of the creation and annihilation operator can be written as:

$$V = -\sum_k (\hat{e}_k \cdot P) \frac{e}{m} \left(\frac{2\pi h}{\omega_k L^3}\right)^{1/2} (\hat{a}_k^+ + \hat{a}_k) \tag{1-13}$$

$$\text{so} \quad \omega_{if}^{(1)} = \frac{4\pi^2 \omega_L}{\hbar L} \sum_i \sum_f |\hat{e}_i \cdot \mu_{fi}|^2 \delta(\omega_{fi} - \omega_l) \tag{1-14}$$

The OPA oscillator strength of an electronic transition from the ground state (0) to the final state (f) can be obtained by

$$f_{0f} = \frac{8\pi^2}{3} \frac{m_e}{e^2 h} v_{0f} |\mu_{0f}|^2 \tag{1-15}$$

where, m_e is the electron mass, e is the electron charge, h is Planck's constant, $v_{0f} = E_{0f}/h$ is the frequency in s^{-1} corresponding to the transition energy (E_{0f}) between the two states, and the transition dipole moments are given by

$$\mu_{0f} = \langle 0 | er | f \rangle \tag{1-16}$$

The computed oscillator strength is related to the experimental integrated intensity by

$$f_{0f} = 4.32 \times 10^{-9} \int \in (\bar{v}) \mathrm{d}\bar{v} \tag{1-17}$$

where, $\in$ is the extinction coefficient in unit $L \cdot mol^{-1}$, and $\bar{v}$ is the frequency in cm^{-1}. Since the integration limits in Eq. (1-3) are generally not known, a single Gaussian (or Lorentzian) function is often used to represent an experimental spectral band, which gives rise to an approximate measure of the corresponding band intensity. Using a Gaussian line-shape

$$f_{0f} = 4.32 \times 10^{-9} \in_{\max} \int e^{-(\Delta\bar{v}/\theta)^2} \mathrm{d}\bar{v} = 4.32 \times 10^{-9} \sqrt{\pi} \in_{\max} \theta \tag{1-18}$$

The θ width parameter relates to the full width (W) at half maximum ($\in_{\max}/2$) by $W = 2 (\ln 2)^{1/2} \theta$, and the cross section (in cm^2) at the band maximum relates to $\in_{\max}$ by $\sigma_{\max} = 3.83 \times 10^{-21} \in_{\max}$ Thus, $\in_{\max}$ or $\sigma_{\max}$ of a transition can be readily approximated, provided its bandwidth is known.

References

[1] SKOTHEIM T. Handbook of conducting polymers[M]. Ⅰ, Ⅱ. New York: Marcel Dekker, 1986.

[2] CHEMLA D S, ZYSS J. Nonlinear optical properties of organic molecules and crystals academic[M]. New York: Elsevier, 1987.

[3] PRASAD P N, WILLIAMS D J. Introduction to nonlinear optical effects in molecules and polymers[M]. New York: Wiley, 1991.

[4] VIVAS M G, NOGUEIRA S L, SILVA S H, et al. Linear and nonlinear optical properties of the thiophene/phenylene-based oligomer and polymer[J]. Phys. Chem. B, 2011, 115(44): 12687-12693.

[5] YOON Z S, KWON J H, YOON M C, et al. Nonlinear optical properties and excited-state dynamics of highly symmetric expanded porphyrins[J]. Am. Chem. Soc., 2006, 128(43): 14128-14134.

[6] NGUYEN K A, ROGERS J E, SLAGLE J E, et al. Effects of conjugation in length and dimension on spectroscopic properties of fluorene-based chromophores from experiment and theory[J]. Phys. Chem. A, 2006, 110(49): 13172-13182.

[7] GRÄTZEL M. Dye-sensitized solar cells[J]. Journal of Photochemistry and Photobiology C: Photochemistry Reviews, 2003, 4: 145-153.

[8] YOU J B, DOU L T, KEN Y, et al. A polymer tandem solar cell with 10.6% power conversion efficiency[J]. Nat Commun., 2013, 4: 1446.

[9] DVORNIKOV A S. Rentzepis[J]. Science, 1989, 245: 843.

[10] DENK W, STRICKLER J H, WEBB W W. Two-photon laser scanning fluorescence microscopy[J]. Science, 1990, 248(4951): 73-76.

[11] KATHARINE G, TAO Y F, SEGALMAN R A, et al. Synthesis and characterization of fluorinated heterofluorene-containing donor-acceptor aystems[J]. Org. Chem., 2010, 75(6): 1871-1887.

[12] WARD J F. Calculation of nonlinear optical susceptibilities using diagrammatic perturbation theory[J]. Reviews of Modern Physics, 1965, 37(1): 1.

[13] ORR B J, WARD J F. Perturbation theory of the non-linear optical polarization of an isolated system[J]. Molecular Physics, 1971, 20(3): 513-526.

[14] LANGHOFF P W, EPSTEIN S T, KARPLUS M. Aspects of time-dependent perturbation theory[J]. Reviews of Modern Physics, 1972, 44(3): 602.

[15] TRETIAK S, CHERNYAK V. Resonant nonlinear polarizabilities in the time-dependent density functional theory[J]. The Journal of Chemical Physics, 2003, 119 (17): 8809-8823.

CHAPTER 2

Charge Transfer and Electron-Hole Coherence in OPA

Photoinduced charge transfer (CT) from donor to acceptor is a primary step in photophysical, photochemical as well as photobiological processes[1-5]. The CT process can be intermolecular, in which an electron is transferred from electron-donating species (D) to electron-accepting species (A), producing the radical cation of donor and the radical anion of acceptor, or intramolecular CT, involving charge redistribution in the excited molecule which produces a very large excited state dipole moment. It is well known that photophysical properties of the organic molecules are determined predominantly by the low energy excited states. Knowledge of nature of excited states, and interplay of inter- and intra- molecular mechanism in the CT process, are becoming very important to develop the novel optoelectronic devices.

Quantum chemistry provides practical approaches for studies on excited states. Upon OPA, the singlet excited states $|S_n\rangle$ are represented by vectors $\boldsymbol{C}^{\mathrm{CI}}_{n,ai}$ based on configurations of unoccupied and occupied molecular orbitals $\boldsymbol{a}$ and $\boldsymbol{i}$, respectively. The molecular orbitals are in turn given by linear combinations of atomic orbitals (LCAOs) μ and ν with coefficients $c^{\mathrm{LCAO}}_{a\mu}$ and $c^{\mathrm{LCAO}}_{i\nu}$. In order to characterize the excited state by observables we define two matrices[6,7]:

$$\begin{cases} \boldsymbol{Q}^{(n)}_{\mu\nu} = \dfrac{1}{\sqrt{2}} \displaystyle\sum_{\substack{a\in \text{unocc} \\ i\in \text{occ}}} \boldsymbol{C}^{CI}_{n,ai} \left(c^{\mathrm{LCAO}}_{a\mu} c^{\mathrm{LCAO}}_{i\nu} + c^{\mathrm{LUAO}}_{i\mu} c^{\mathrm{LCAO}}_{a\nu} \right) \\ \boldsymbol{P}^{(n)}_{\mu\nu} = \dfrac{\mathrm{i}}{\sqrt{2}} \displaystyle\sum_{\substack{a\in \text{unocc} \\ i\in \text{occ}}} \boldsymbol{C}^{CI}_{n,al} \left(c^{\mathrm{LCAO}}_{a\mu} c^{\mathrm{LCAO}}_{i\nu} - c^{\mathrm{LCAO}}_{i\nu} c^{\mathrm{LCAO}}_{a\nu} \right) \end{cases} \tag{2-1}$$

which are (anti)symmetric for exchange of the atomic orbitals and normalized as

$$\sum_{\mu,\nu} |\boldsymbol{Q}^{(n)}_{\mu\nu}|^2 = \sum_{\mu,\nu} |\boldsymbol{P}^{(n)}_{\mu\nu}|^2 = 1 \tag{2-2}$$

试读结束：需要全本请在线购买： www.ertongbook.com

In the collective electron oscillator (CEO) model[8] the excited state $|S_n\rangle$ is described by a harmonic oscillator with oscillating coordinate $\boldsymbol{Q}_{\mu\nu}^{(n)}\cos(\omega_n t)$ and momentum $\boldsymbol{P}^{(n)}\sin(\omega_n t)$ for the transition frequency ω_n. For visual characterization of the excited states we use two different representations of the matrices $\boldsymbol{Q}_{\mu\nu}^{(n)}$ and $\boldsymbol{P}_{\mu\nu}^{(n)}$.

1. Real-space representation

In real space the oscillating CEO coordinate and momentum are given as[6,7]

$$\begin{cases} Q_n(r,r';t) = \sum_{\mu\nu}\phi_\mu^{AO}(r)\boldsymbol{Q}_{\mu\nu}^{(n)}\phi_\nu^{AO}(r')\cos(\omega_n t) \\ P_n(r,r';t) = \sum_{\mu\nu}\phi_\mu^{AO}(r)\boldsymbol{P}_{\mu\nu}^{(n)}\phi_\nu^{AO}(r')\sin(\omega_n t) \end{cases} \tag{2-3}$$

The diagonal slice for $r = r'$ results in

$$\begin{cases} Q_n(r,r;t) = \sqrt{2}\rho_{n0}(r)\cos(wt) \\ P_n(r,r;t) = 0 \end{cases} \tag{2-4}$$

The amplitude of the former is given by the so-called transition density (TD):

$$\rho_{n0}(r) = \frac{1}{\sqrt{2}}\sum_{\mu,\nu}\phi_\mu^{AO}(r)Q_{\mu\nu}^{(n)}\phi_\nu^{AO}(r) \tag{2-5}$$

The transition density contains information about the spatial location of the excitation[9] and is directly related to the transition dipole

$$\mu_{n0}(r) = e\int r\rho_{n0}(r)\mathrm{d}^3 r \tag{2-6}$$

Furthermore, it is of particular relevance for excitonic interaction at shorter distances[10]. Besides the transition density, the charge difference density (CDD)

$$\Delta\rho_m(r) = 2i\sum_{\mu,\nu,k}\phi_\mu^{AO}(r)Q_{k\mu}^{(n)}P_{k\nu}^{(n)}\phi_\nu^{AO}(r) \tag{2-7}$$

is another useful quantity for real-space characterization of excitons. It represents the difference of electron distribution between the excited state $|S_n\rangle$ and the ground state $|S_0\rangle$. In the present work, both transition and charge difference densities are represented by isosurfaces based on a 3D grid of approximately 100 000 cubes.

2. Site representation

For site representations of the CEO coordinate and momentum, we define them as:

$$\overline{\boldsymbol{Q}_{AB}^{(n)2}} = \sum_{\substack{\mu\in A\\ \nu\in B}} \left|\boldsymbol{Q}_{\mu\nu}^{(n)}\right|^2, \quad \overline{\boldsymbol{P}_{AB}^{(n)2}} = \sum_{\substack{\mu\in A\\ \nu\in B}} \left|\boldsymbol{P}_{\mu\nu}^{(n)}\right|^2 \tag{2-8}$$

respectively[8,11]. This means that the matrices $\boldsymbol{Q}_{\mu\nu}^{(n)}$ and $\boldsymbol{P}_{\mu\nu}^{(n)}$ are merged for atomic orbitals μ and ν belonging to atomic sites A and B, respectively. Thus $\overline{\boldsymbol{P}_{AB}^{(n)2}}$ gives the atomic sites A and B where electron and hole oscillate from and to, while $\overline{\boldsymbol{Q}_{AB}^{(n)2}}$ is a measure of the delocalization of the exciton as a whole. Note that for Frenkel excitons the occupation of $\overline{\boldsymbol{Q}_{AB}^{(n)2}}$ and $\overline{\boldsymbol{P}_{AB}^{(n)2}}$ is limited. to pairs of atomic centers A and B belonging to the same monomeric unit.

References

[1] BRÉDAS J L, BELJONNE D, COROPCEANU V, et al. Charge-transfer and energy-transfer processes in π-conjugated oligomers and polymers: a molecular picture[J]. Chemical Reviews, 2004, 104(11): 4971-5004.

[2] MATAGA N, CHOSROWJAN H, TANIGUCHI S. Ultrafast charge transfer in excited electronic states and investigations into fundamental problems of exciplex chemistry: our early studies and recent developments[J]. Journal of Photochemistry and Photobiology C: Photochemistry Reviews, 2005, 6(1): 37-79.

[3] FU H B, YAO J N. Size effects on the optical properties of organic nanoparticles[J]. Journal of the American Chemical Society, 2001, 123(7): 1434-1439.

[4] ZHAO G J, CHEN R K, SUN M T, et al. Photoinduced intramolecular charge transfer and S2 fluorescence in thiophene-π-conjugated donor-acceptor systems: experimental and TDDFT studies[J]. Chemistry-A European Journal, 2008, 14(23): 6935-6947.

[5] CHO D W, FUJITSUKA M, YOON U C, et al. Intermolecular photoinduced electron-transfer of 1, 8-naphthalimides in protic polar solvents[J]. Physical Chemistry Chemical Physics, 2008, 10(30): 4393-4399.

[6] WANG C, KILITZIRAKI M, MACBRIDE J A H, et al. Tuning the optoelectronic properties of pyridine—containing polymers for light—emitting devices[J]. Advanced Materials, 2000, 12(3): 217-222.

[7] KIM J K, YU J W, HONG J M, et al. An alternating copolymer consisting of light emitting and electron transporting units[J]. Journal of Materials Chemistry, 1999, 9 (9): 2171-2176.

[8] MUKAMEL S, TRETIAK S, WAGERSREITER T, et al. Electronic coherence and collective optical excitations of conjugated molecules[J]. Science, 1997, 277(5327): 781-787.

[9] JESPERSEN K G, BEENKEN W J D, ZAUSHITSYN Y, et al. The electronic states of polyfluorene copolymers with alternating donor-acceptor units[J]. The Journal of

Chemical Physics, 2004, 121(24): 12613-12617.

[10] BEENKEN W J D, PULLERITS T. Excitonic coupling in polythiophenes: comparison of different calculation methods[J]. The Journal of Chemical Physics, 2004, 120(5): 2490-2495.

[11] ZOJER E, BUCHACHER P, WUDL F, et al. Excited state localization in organic molecules consisting of conjugated and nonconjugated segments[J]. The Journal of Chemical Physics, 2000, 113(22): 10002-10012.

CHAPTER 3

Application of OPA

3.1 Biology

3.1.1 Retinal proteins (rhodopsins)

Rhodopsins are located in cell membrane and eye retina, which naturally exist in protonated Schiff-base form and can convert EM energy into chemical one[1]. The absorption of visible light that strikes eyes can arouse in the molecule an ultrafast response. As a central issue in photobiology, understanding the intrinsic ultrafast response mechanism is a challenging work[2,3]. Because most experiments[4-6] were performed in liquid phases till the recent papers[2,3], it is hard to decide if the ultrafast response is an intrinsic property of this class molecules or a consequence of an interaction between the molecule and environment[7,8]. Theoretically, Anfinrud[9] and co-workers have suggested a three-state (S_0, S_1 and S_2) model to explain the ultrafast photophysics process in bacteriorhodopsin. Olivucci[10] and co-workers proposed another two-state (S_0 and S_1) model and studied the related isomerization pathways on the S_1 and S_2 states in solution phase[11] and concluded that S_1 and S_2 are nearly degenerate states, which is similar to the conclusion drawn by Yamamoto[12] et al. Moreover, the S_1-S_2 level spacing is sensitive to the external perturbations and the measurements in different conditions[4-6,13-15], and the addition of solutions makes the situation more complicated. Therefore, the S_1 and S_2 excited states' behavior in the vacuum and unperturbed conditions are very important for extracting the ultrafast response mechanism hidden in the veil.

As a specific example of retinal protein, the photoisomerization from 11-*cis*

protonated Schiff base (PSB11) to its all *trans* protonated Schiff base (PSBT) isomer (see Fig. 3-1 for their structures) is one of the fastest chemical reactions observed so far[7,16]. Some experimental[4-6] and theoretical[11,17] studies have been reported in different solutions for understanding such a phenomenon. As a result of low target densities, few experiments were done in the gas phase. However, information related to this photoisomerization process without external perturbations is crucial for elucidating the mechanism, since it can provide us a simpler picture about the photophysical and photochemical processes than ones in solution phase[2,3]. In this work, the T_v, f and μ values of the PSB11 and PSBT for S_1 and S_2 excited states were calculated by time-dependent density functional theory (TD-DFT) methods in vacuum and compared with the experimental detected values[2]. The experimentally observed phenomenon that the S_2 μ value is much smaller than the S_1 one was interpreted by a 3D representation of transition densities. The different optical behaviors (linear and nonlinear optical responds) of the excited states were investigated by considering different strengths of external electric fields.

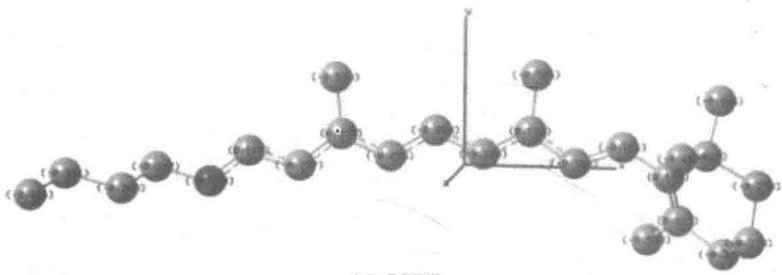

(a) PSBT

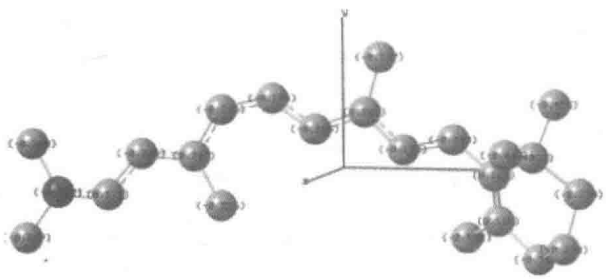

(b) PSB11

Figure 3-1 The schematic structure of (a) PSBT and (b) PSB11 retinal chromophores without H atoms together with the coordinate systems

The PSB11 ground state geometry was optimized by the B3LYP method with 6-31G-(d), 6-31 + G(d) and 6-311 ++ G(d) basis sets. The results indicated that the size of the basis sets hardly affect the geometric parameters. Then PSBT ground-state geometry was just optimized by B3LYP/6-31G(d) and B3LYP/ 6-31 + G(d), which also showed that the basis set size hardly influences the optimization results. Hereafter, the property calculations of PSB11 and PSBT were performed under their B3LYP/6-31G-(d) optimized ground-state geometries. The subsequent B3LYP/6-31G(d) and B3LYP/6-31 + G(d) frequency analyses indicated that the optimized geometries are the total minima on the potential energy surface of PSB11 and PSBT, respectively.

Table 3-1 shows S_1 and S_2 vertical excitation energies and oscillator strengths. The T_v and f values of the PSBT and PSB11 for S_1 and S_2 states were calculated by TD-B3LYP, TD-BPW91 and TDSVWN along with 6-31G (d), 6-31 + G(d) and 6-311 ++ G(d) basis sets, respectively. The calculated results were compared with the experimental detected values. For both PSBT and PSB11, the basis set size has very little affect on the calculated T_v and f values. However, the different functionals of the TD-DFT method do affect the calculated T_v and f values. For the PSBT S_1 and S_2 states, the TD-B3LYP, TD-BPW91 and TD-SVWN with 6-31G(d) basis set calculated $T_v(f)$ values to be 536.1(1.561)nm and 393.7(0.669)nm, 590.5(0.835)nm, 451.9(0.891) nm, 592.3(1.003) nm and 451.1(1.058) nm, respectively.

Table 3-1 TD-B3LYP and TDA calculated transition energies (in nm) of the first two excited states of PSBT and PSB11, compared with the corresponding experimental values

Method	PSBT		PSB11	
	S_1	S_2	S_3	S_4
Exp.	620	385	610	390
TD-B3LYP/6-31G(d)	536.1	393.7	539.5	396.8
	(1.561)	(0.669)	(1.228)	(0.577)
TD-B3LYP/6-31+G(d)	543.1	397.3	546.6	400.0
	(1.580)	(0.647)	(1.295)	(0.564)
TD-B3LYP/6311++G(d)	543.9	398.1	548.1	401.3
	(1.579)	(0.646)	(1.291)	(0.561)
TD-BPW91/6-31G(d)	590.5	451.9	590.5	451.9
	(0.835)	(0.891)	(0.835)	(0.891)

试读结束：需要全本请在线购买： www.ertongbook.com